Characterizing the Motogenic Response of Human Keratinocytes to Epidermal Growth Factor and Transforming Growth Factor-Alpha

by

Stephen D. Rodgers

B.S. Chemical Engineering
Lehigh University, 1994

Submitted to the Department of Chemical Engineering in partial fulfillment of the requirements for the degree of

Master of Science in Chemical Engineering

at the

Massachusetts Institute of Technology

September 1996

Signature of Author .....
Department of Chemical Engineering
July 31, 1996

Certified by .....
Douglas A. Lauffenburger
Professor of Chemical Engineering
Thesis Supervisor

Accepted by .....
Robert E. Cohen
Professor of Chemical Engineering
Chairman, Committee for Graduate Studies

Characterizing the Motogenic Response of Human Keratinocytes to Epidermal Growth Factor and Transforming Growth Factor-Alpha

by

Stephen D. Rodgers

Submitted to the Department of Chemical Engineering on July 31, 1996, in partial fulfillment of the requirements for the degree of Master of Science in Chemical Engineering

Abstract

Experiments were performed to quantitatively characterize the differential migratory response of human keratinocytes to the polypeptide growth factors EGF and TGF-α. Videomicroscopic tracking of single cells, on collagen IV surfaces, was used to examine the migratory response of cells to a range of growth factor concentrations, as well as to the EGF receptor blocking antibody 225. Results indicate that both EGF and TGF-α increase the random motility coefficient of human keratinocytes, relative to control experiments and those in which EGFR blocking antibody is used. This increase in motility appears to occur in a dose-dependent manner, with TGF-α performing as a stronger motogen than EGF. Results also suggest that the addition of exogenous growth factor or receptor blocking antibody lowers cellular persistence times relative to the control state. This finding supports a model of autocrine pathways as cellular environmental sensing systems, a model that has been termed "cell sonar".

Thesis Supervisor: Douglas A. Lauffenburger
Title: Professor

Acknowledgements

I would like to thank my advisor, Doug Lauffenburger, for his advice, encouragement, and support throughout the course of this work. My tenure at M.I.T. has taken some interesting turns, and I appreciate the understanding he has shown along the way. Thanks also go to everyone in the Lauffenburger group for providing an enjoyable atmosphere in which to work, and without whose patience I may never have improved my cell culture techniques. Additional thanks to Gargi Maheshwari, Sean Palecek, Cartikeya Reddy, and Marti Ware for many insightful discussions on the theoretical and statistical analysis of experimental data. Finally, many thanks to Jenny and my entire family for their continued support of all my endeavors.

Contents

List of Figures

Chapter 1

Introduction and Background

1.1 The Epidermal Growth Factor Receptor and its Cognate Family of Ligands

The epidermal growth factor receptor (EGFR) is arguably the most thoroughly characterized member of the receptor tyrosine kinase family of signaling molecules. This 175 kDa, single chain, transmembrane glycoprotein is composed of 1186 amino acids and N-linked carbohydrates (Pimentel, 1994). As shown in Figure 1, the receptor has a 621 amino acid extracellular ligand binding domain, a 22 amino acid transmembrane region, and a 542 amino acid intracellular domain. Furthermore, the intracellular region is comprised of both a tyrosine kinase and a regulatory domain (Chang et al., 1993). All of the several intracellular signaling cascades that can be activated by the EGFR, upon binding of a cognate ligand, depend in part on the successful dimerization of receptors and autophosphorylation of intracellular tyrosine residues. Subsequent to autophosphorylation events, SH2 domains on other intracellular proteins involved in signaling pathways, such as PLC-γ, GAP, SHC, and GRB-2, interact with these phosphotyrosine moieties. It is the interaction of SH2 domains with any of the five intracellular tyrosine residues of the EGFR that allows the receptor to participate in many important signaling pathways (reviewed by van der Geer et al., 1994).

The physiological importance of the EGFR is highlighted by its presence on numerous cell types (Carpenter and Wahl, 1990; Gospodarowicz, 1981) and the variety of responses it is capable of eliciting. The actual outcome of receptor activation is a function of tissue location and state of differentiation of the host cell (Khazaie et al., 1993), however the EGFR has been shown to participate in the stimulation of cell proliferation, gene induction, differentiation, and migration (Barrandon and Green, 1987; Carpenter and Wahl, 1990; Hudson and Gill, 1991; Wells, 1988). In addition to its role in normal physiology and development, the EGFR is also involved in the dysregulation of cell function. EGFR expression and activity are associated with several pre-malignant and malignant pathologies including benign hyperplasia of the skin, mammary carcinoma, glioblastoma, and hepatic carcinoma (Khazaie et al., 1993). Indeed, the EGFR is the receptor most commonly implicated in the pathology of all human cancers (Aaronson, 1991).

Each member of the epidermal growth factor (EGF) family of ligands, which also includes amphiregulin, betacellulin, heparin-binding EGF (HB-EGF), and transforming growth factor-alpha (TGF-α), is capable of independently binding to and activating the EGFR (Soler and Carpenter, 1994). The two most thoroughly characterized members of this family are EGF and TGF-α. Both molecules are initially synthesized as transmembrane precursors (Soler and Carpenter, 1994), and they share a 42% amino acid sequence homology, a major consequence of which is similar binding affinities to the EGFR (Burgess, 1989; Lee et al., 1995; Massague, 1983). The dissociation constant (K_D) for both receptor/ligand interactions has been experimentally determined to be approximately 2 nM (Ebner and Derynck, 1991). Although information

regarding the processing pathway of the precursor EGF molecule is limited, the mature form, a 6 kDa, 53 amino acid, single polypeptide chain, is known to originate from a transmembrane precursor that may be as large as 128 kDa (Carpenter and Cohen, 1990; Gray et al., 1983; Massague and Pandiella, 1993). TGF-α is synthesized as a 160 amino acid precursor (Bringman et al., 1987), but some cells cleave this precursor molecule to form several membrane associated, as well as soluble species, including the mature form, a 6 kDa, 50 amino acid soluble polypeptide (Massague, 1990). In contrast to the transmembrane precursor of EGF, for which there is no indication of biological activity (Burgess, 1989), both the precursor and mature form of TGF-α are able to bind to and activate the EGFR (Brachmann et al., 1989; Wong et al., 1989).

EGF and TGF-α are known to stimulate a variety of cell types, including almost all fibroblasts, epithelia, and muscle cells (Burgess, 1989), and both ligands have been shown to stimulate cell migration (Bade and Nitzgen, 1985; Barrandon and Green, 1987; Cha et al., 1996), proliferation (Barrandon and Green, 1987), wound healing (Schultz et al., 1987), neurite extension (Manske and Bade, 1994), and angiogenesis (Schreiber et al., 1986). Physiologically, EGF is known only to be released by cells in the salivary gland (Ebner and Derynck, 1991), whereas TGF-α is known to be produced in macrophages (Madtes et al., 1988; Rappolee et al., 1988), the brain (Wilcox and Derynck, 1988), the pituitary (Kobrin et al., 1988), and many types of epithelia (Beauchamp et al., 1989; Coffey et al., 1987; Valverius et al., 1989). Under normal conditions, epithelial cells are the major source of TGF-α synthesis (Derynck, 1992). Because these cells also express the EGFR on their surface (Carpenter and Wahl, 1990), overproduction of TGF-α is directly related to many neoplasias and

hyperproliferative disorders, particularly in human keratinocytes (Bates et al., 1988; Derynck et al., 1987; Dominey et al., 1993; Nister et al., 1988).

1.2 Cell Migration

Cell migration is an important process that occurs in many aspects of normal physiology and development, as well as pathology. Examples include the formation of nervous system structures, a result of the outward migration of neurons from the neural crest, the movement of neutrophils scavenging antigenic material, bone remodeling, and the metastasis of tumor cells. More familiar evidence of this phenomenon is seen in the wound healing process, during which a progression of immune cells, fibroblasts, and epithelial cells interact so as to renew the structure of damaged tissue (reviewed by Clark, 1993). Keratinocytes play a pivotal role during the reepithelialization stage of the wound healing process, moving on the order of hours after injury to close the wound surface and restore the skin's barrier function (Winter, 1962). These cells express the EGFR on their surface, as well as produce both TGF-α and HB-EGF (Derynck, 1992; Hashimoto et al., 1994; Pittelkow et al., 1993). This autocrine pathway makes examining the migratory response of keratinocytes to EGFR ligand a more complex issue.

1.3 The Differential Cellular Response Elicited by Epidermal Growth Factor and Transforming Growth Factor-Alpha

In spite of their similarities, EGF and TGF-α are capable of evoking differential cellular responses (Barrandon and Green, 1987; Cha et al., 1996; Ebner and Derynck, 1991; Reddy et al., 1996b; Schreiber et al., 1986). Specifically, in assays measuring the stimulatory effect of the two ligands on

keratinocyte migration, as well as the ability to modulate *in vitro* wound closure, TGF-α displayed stronger motogenic properties than EGF (Cha et al., 1996). A possible explanation for this effect, one that does not necessitate differential signaling, is the difference in isoelectric points of the two molecules (Ebner and Derynck, 1991). This biochemical difference manifests itself as a variation in the pH sensitivity of the binding affinities of the two ligands for the EGFR (Ebner and Derynck, 1991; French et al., 1995). At a lower pH, such as that found in the intracellular vesicles in which the internalized growth factor-receptor complex is located, the K_D for the TGF-α /EGFR interaction increases approximately twice as much as that of EGF/EGFR interaction (French et al., 1995). This variation in binding affinity has significant implications for the intracellular processing pathways of both ligand and receptor (Reddy et al., 1996b). As a result of the higher intracellular K_D, relative to EGF, TGF-α dissociates from the EGFR to a much greater extent than EGF. Therefore, in accordance with an understanding of the mechanisms of endosomal sorting (French and Lauffenburger, 1996), the uncoupled TGF-α ligand is degraded to a greater extent than EGF. Additionally, a greater fraction of receptors recycles to the cell surface when internalized with the TGF-α molecule than when internalized via an EGF/EGFR complex (Ebner and Derynck, 1991; Reddy et al., 1996b). A critical examination of EGF and TGF-α trafficking dynamics in fibroblasts has demonstrated that the proliferative response to stimulation by these ligands is not straight forward. In fact, three regimes of behavior (discussed in chapter 4) were seen (Reddy et al., 1996b). Whether mechanisms governing cell migration are controlled in the same manner is unclear.

1.4 Thesis Overview

This work brings a rigorously quantitative approach to the analysis of human keratinocyte migration, for the purpose of elucidating differential effects that EGF and TGF-α exert on cell migratory behavior. The stimulatory effects of a range of concentrations of exogenously applied EGF and TGF-α were examined, as well as the inhibitory effect of EGFR blocking antibody. Experimental data indicate that both ligands increase the random motility coefficient of human keratinocytes, relative to control experiments and those in which EGFR blocking antibody is used. This increase in motility appears to occur in a dose-dependent manner, with TGF-α performing as a stronger motogen than EGF. This result is in agreement with predictions one would make concerning the performance of these ligands, based upon a consideration of their trafficking properties. Persistence time data reveal another interesting feature of the cells. Consistent with a model of autocrine secretion as a method of cell sonar, results suggest that disruption of native autocrine loops through the addition of exogenous growth factor or receptor blocking antibody lowers persistence times relative to the control state in which no perturbations in autocrine loops are introduced.

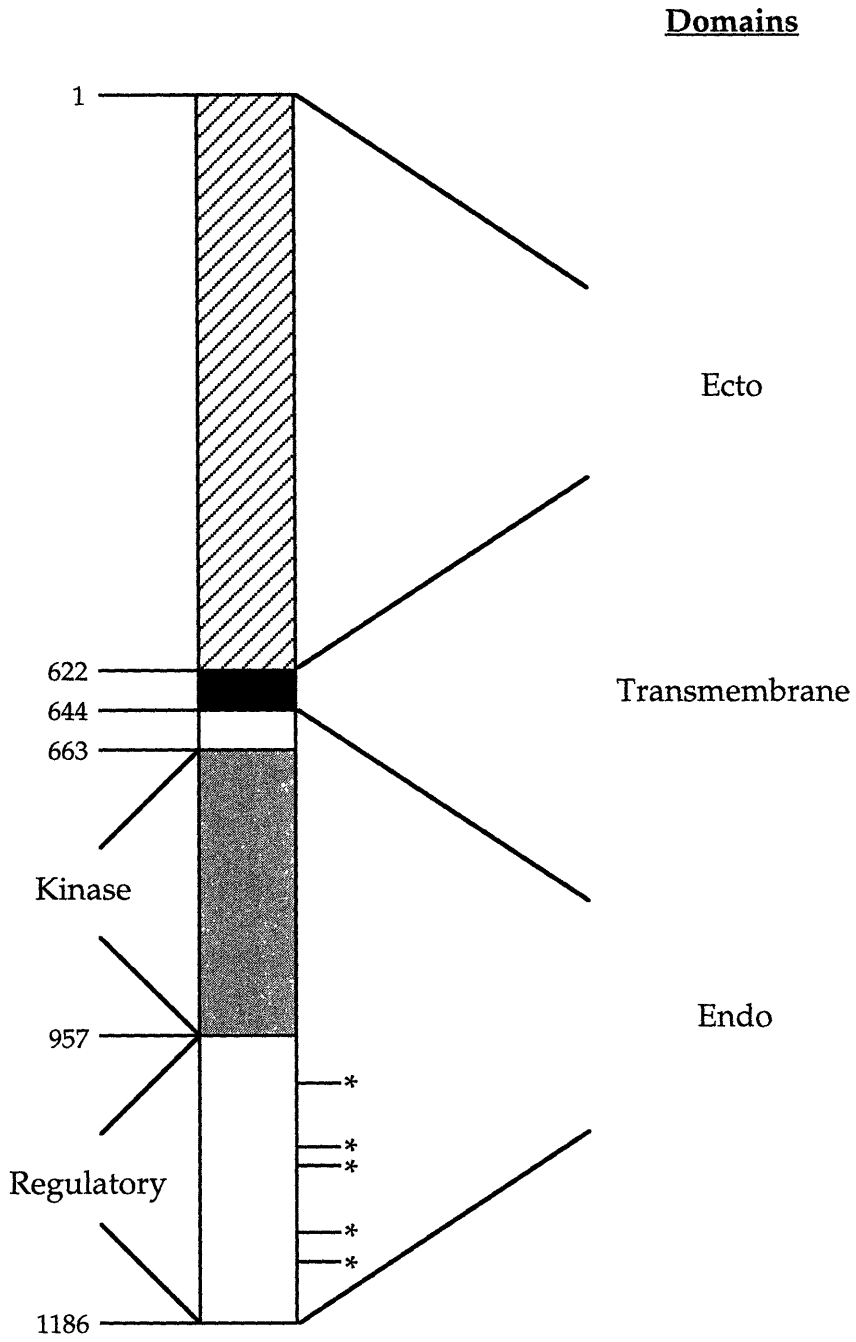

Figure 1 The EGF receptor (from Chang et al., 1993). Asterisks indicate sites of tyrosine phosphorylation.

Chapter 2

Materials and Methods

2.1 Cell Culture

Normal human epidermal keratinocytes, derived from neonatal foreskins and cultured under serum-free conditions in standard formulation keratinocyte serum-free medium (KSFM, Gibco BRL, Grand Island, NY), were a generous gift from Dr. Laurie Hudson (Northwestern University). Cells were maintained in 25 cm^2 tissue culture flasks. For routine maintenance of keratinocytes, media was supplemented with EGF and bovine pituitary extract (supplied by the vendor along with the KSFM), as well as 0.1% w/v bovine serum albumin (BSA), 100 units/mL penicillin, and 100 μg/mL streptomycin antibiotics. Media for experiments involving the addition of growth factors consisted of KSFM, 0.1% w/v BSA, antibiotics, and the appropriate amount of human recombinant EGF or TGF-α (Gibco BRL, Grand Island, NY). A starve media, composed only of KSFM and 0.1% w/v BSA, was prepared for the maintenance of cells 24 hours prior to the start migration experiments.

In passaging and seeding cells, a mixture of 0.25% trypsin and 1 mM EDTA (Gibco BRL, Grand Island, NY) was used. Upon detachment, ion-free PBS (Sigma, St. Louis, MO) was added, and the mixture was centrifuged for approximately 3 minutes at 800-1000 rpm. After centrifugation, the

supernatant was discarded, and the cells were resuspended in routine media. Cells were then passaged or counted in a hemocytometer in preparation for seeding. In the latter case, cell viability was assessed using trypan blue stain. Only cells of passage 9 and lower were used in experiments.

2.2 Migration Assay Protocols

Experiments were conducted in 35 mm tissue culture dishes coated with collagen IV (Biocoat Plates, Becton Dickonson/Collaborative Biomedical, Bedford, MA), a large, network forming protein which is the primary constituent of basement membranes (Yaoita et al., 1978). For all experiments, approximately 2500 cells were seeded and allowed to attach overnight in routine media. This low cell density minimized the possibility of cell/cell interactions throughout the course of experiments. Following the initial attachment period, cells were given starve media for 24 hours. At the start of control experiments, dishes were replenished with 4 mL of starve media. At the start of experiments involving the addition of growth factors, dishes were replenished with 4 mL of the appropriate growth factor-containing media.

For experiments involving the use of the monoclonal antibody 225 (mAb 225), a 20 nM concentration of antibody in starve media was added to cells. 225 is a clone that specifically binds to the EGFR, inhibiting the binding of cognate ligands (Kawamoto et al., 1983; Sato et al., 1983). Its K_D for the EGFR has been reported as 0.6-1.3 nM (Sato et al., 1987). For these experiments, cells were incubated in a 20 nM concentration of antibody in starve media for 24 hours, followed by replenishment with 4 mL of the antibody-containing media at the start of the tracking experiment.

2.3 Migration Assay Specifications

Motility assays were based on the method of single cell tracking (DiMilla et al., 1992). After starving cells for 24 hours and replenishing with the appropriate media, petri dishes were placed into the insert of a motorized stage on a Zeiss Axiovert 100 inverted microscope (stage and insert from LUDL electronics, Hawthorne, NY). Cells were viewed using a 10X objective with phase contrast optics. Physiological conditions were maintained on the stage in two ways. To maintain temperature, warm water was circulated around the dish, through ports on the stage insert. To maintain pH and humidity, a humidified air/CO_2 mixture was perfused over the dish, through an additional port on the stage insert. To expedite the acquisition of data from a single experiment, a stage controller (nuLogic Inc., Needham, MA) and appropriate software (Labview, National Instruments, Bloomfield, CT) were used to control the timing and positioning of the motorized stage. Up to 25 fields were selected at random for each experiment, and each of these user designated positions was then visited for approximately 30 seconds, every 15 minutes, for the duration of the experiment. Experiments were run for as long as 24 hours, but no shorter than 10 hours. Approximately 40 cells were followed per experiment. Time-lapse images of each experiment were recorded at 1/480th of real time using a Hitachi KP-M1 CCD camera and Panasonic AG-6720A time-lapse VCR (RPI, Wayland, MA). Only images taken at least 30 minutes after the addition of growth factor-containing media were used for analysis.

2.4 Data Analysis and Acquisition

Cell centroids as a function of time were acquired from video recordings of cell tracking experiments. Tapes were played back on a Panasonic AG-1980 VCR with built-in time-base corrector (Crimson Tech, Cambridge, MA), through a Power Macintosh 8500 with a Scion VG-5 frame grabber card (Scion Corp., Frederick, MD). Using image analysis software (NIH Image), pixel coordinates of individual cell centroids were acquired from the video images by manually forwarding the tape and selecting cells of interest with the mouse. Individual fields were followed over time by forwarding the tape at appropriate intervals, a process that was hastened by the presence of a time/date stamp recorded on the images from all experiments. Pixel coordinates were stored in a data file to be used for further analysis.

To analyze cell paths thus acquired, several data manipulations were required. Due to an offset in stage positioning, stage drift was seen in many of the experiments. This phenomenon, which can be seen in cell tracks that appear as straight, parallel lines, was corrected for in the data analysis. Using cells that exhibited stage drift as their only motion, a drift rate was calculated in both the x and y direction. The individual cell drift rates were then averaged over all cells exhibiting this behavior to determine an average drift rate in both directions. Using average drift rate information, the stage drift was subtracted from the (x,y) positions of all cells for a given experiment. The transformation is represented mathematically in eqns (2.1-2.4),

$$\Psi_x = \frac{1}{n}\sum_{i=1}^{n}\left(\frac{x_{end} - x_{start}}{\delta}\right)_i \qquad \text{eqn (2.1)}$$

$$\Psi_y = \frac{1}{n}\sum_{i=1}^{n}\left(\frac{y_{end} - y_{start}}{\delta}\right)_i \qquad \text{eqn (2.2)}$$

$$x_{corrected} = x_{uncorrected} - \Psi_x \int_0^{\tau} dt \qquad \text{eqn (2.3)}$$

$$y_{corrected} = y_{uncorrected} - \Psi_y \int_0^{\tau} dt \qquad \text{eqn (2.4)}$$

where Ψ_x and Ψ_y represent the average drift rates in the x and y direction, x_{start}, y_{start}, x_{end}, and y_{end} are the pixel coordinates of a given cell at the beginning and end of an experiment, d represents the total time course of the experiment, n is the number of cells in the experiment exhibiting this behavior, and t is the incremental time course of an experiment.

To quantitate cell motility in the most rigorous sense, the migrating cell is modeled as an isolated particle exhibiting a persistent, random walk in a uniform environment. Over short time periods, the cell moves in linear paths, and over longer time periods, the cell path appears completely random in nature. The time periods described are relative to the persistence time, which is described as the time period between significant changes in direction of cell movement. According to this model, the average squared displacement, $\overline{d^2(t)}$ of a migrating cell, for a period of time t, depends on two parameters: the cell speed, S, and persistence time, P. The relationship is described mathematically in eqn (2.5) (Dunn, 1983; Othmer et al., 1988).

$$\overline{d^2(t)} = 2S^2P\left[t - P\left(1 - e^{-t/P}\right)\right] \qquad \text{eqn (2.5)}$$

To obtain values for the parameters S and P which characterize the cell's movement, it is necessary to calculate the average squared displacement as a function of time for individual cell paths. These values are calculated using data that describe the (x,y) position of the cell centroid over the time course of the experiment.

Before calculating the average squared displacement of the cells however, the data was examined for induction effects that might be present due to the administration of growth factor after a 24 hour period of starvation. To assess whether this effect was present, squared displacements for subsequent 15 minute time intervals, $d_{15}^2(t)$, were calculated for every cell for the duration of each experiment. The values at each time point were then averaged over all cells for which they were computed. The calculations were performed according to eqns (2.6) and eqn (2.7),

$$d_{15}^2(t) = \left\{ [x((i+1)\Delta) - x(i\Delta)]^2 + [y((i+1)\Delta) - y(i\Delta)]^2 \right\} (1.25)^2 \quad \text{eqn (2.6)}$$

$$\underline{d_{15}^2(t)} = \frac{1}{n} \sum_{i=1}^{n} d_{15}^2(t)_i \quad \text{eqn (2.7)}$$

where x and y are the pixel coordinates of the cell centroid, Δ is the 15 minute time interval between successive acquisition of images of each field, 1.25 μm/pixel is a conversion factor obtained using a stage micrometer and the image analysis software, n is the total number of cells tracked for a given experiment, and $\underline{d_{15}^2(t)}$ is the average 15 minute squared displacement as a function of time for the entire cell population. Additionally, the number of cells observed throughout the course of the experiment was examined. In the final data analysis used to calculate speed and persistence, (x,y) data beyond

the time at which the cell population had decreased by more than four cells was discarded. This ensured that a constant population of randomly selected cells was used in the calculation of average squared displacements as a function of time, thus preventing calculations at later times from being biased towards a population of slower moving cells.

Using the transformed data, average squared displacements as a function of time, $\overline{d^2(t)}$, were calculated for each cell using a method of non-overlapping intervals (Dickinson and Tranquillo, 1993). Calculations were performed according to eqns (2.8-2.10).

$$\overline{d^2(t)} = \frac{1}{n_t}\sum_{j=0}^{n_t-1}\left[\left\{\left(x_{(j+1)\Delta} - x_{j\Delta}\right)^2 + \left(y_{(j+1)\Delta} - y_{j\Delta}\right)^2\right\}(1.25)^2\right] \qquad \text{eqn (2.8)}$$

where

$$n_t = \frac{\tau_{\max}}{i\Delta} \quad (i = 1 \rightarrow \Theta) \text{ (largest integer value)} \qquad \text{eqn (2.9)}$$

and

$$\Theta = \frac{\tau_{\max}}{\Delta} \qquad \text{eqn (2.10)}$$

$\tau_{\max}$ is the total length of the experiment, Q is the total number of 15 minute time intervals in the experiment, and n_t is the number of intervals of given time length in the experiment. n_t and the corresponding $\overline{d^2(t)}$ were calculated for each time point by incrementing the index, i, from 1 to Q, in integer values, and calculating the appropriate $\overline{d^2(t)}$. Finally, after calculating the average squared displacement as a function of time for each cell in the

population, an average squared displacement versus time, $\overline{\overline{d^2(t)}}$, was calculated for the entire population, by averaging the values of the individual cells. This is represented mathematically in eqn (2.11).

$$\overline{\overline{d^2(t)}} = \frac{1}{n}\sum_{i=1}^{n}\overline{d^2(t)_i} \qquad \text{eqn (2.11)}$$

In obtaining parameter values, a weighted, nonlinear curve fitting routine was employed. The reciprocal of the standard deviation of the population average squared displacement, $\overline{\overline{d^2(t)}}$, was used for weighting at each time point. The loss function minimized in performing the curve fit is described by eqn (2.12),

$$Loss = \frac{(OBS - PRED)^2}{\sigma} \qquad \text{eqn (2.12)}$$

where PRED is the value of the population average squared displacements as predicted by eqn (2.5), OBS is the experimental value of the population average squared displacements as calculated from the data, and s is the standard deviation of the population average squared displacement at each time point. Weight factors were used to account for non-uniformly distributed residuals in the curve fit, a result of the method of non-overlapping intervals used to calculate such values (Dickinson and Tranquillo, 1993). Error in parameter estimates was determined by fitting the 95% confidence limits on the population average squared displacements to eqn (2.5). The parameter values obtained from these curve fits, along with the parameters characterizing the average squared displacement curve, were

used to calculate a standard error of means for both speed and persistence time.

Chapter 3

Results

3.1 Cell Tracking Data

In preparation for the calculation of average squared displacements as a function of time, cell centroid position data was transformed in several ways. Figure 3.1 shows typical cell tracks obtained from the initial analysis of video images. Stage drift, present in many of the experiments, was removed from the data by applying the transformation described in eqns (2.1-2.4). Typical drift-corrected cell paths are shown in Figure 3.2. In this figure, also called a wind-rose display (Goodman et al., 1989), cell paths are assigned a starting coordinate of (0,0). If a chemotactic gradient, or some other gradient to which cells would respond, were present during the experiments, this type of display would help to identify the preferred direction of motion. As required by the persistent random walk model, the cell paths observed appear to be randomly oriented. Results of calculations designed to look for growth factor induction effects are shown in Figure 3.3. While no initial time course of activation is seen, later times indicate a decrease in average squared 15 minute displacements. As shown in Figure 3.4, by the concomitant decrease in cell number observed over time (for the experiment described in Figure 3.3), the decrease in average squared 15 minute displacements was most likely due to the selection of a slower moving population of cells at later times. Faster

moving cells tend to migrate out from the field of view earlier in experiments than do the slower moving ones, resulting in the undesirable occurrence of a non random population of cells at longer times.

3.2 Average Squared Displacements As a Function of Time

After correcting centroid position data for stage drift and discarding data collected beyond a time in which more than four cells migrated out of the field of view, average squared displacements as a function of time were calculated according to eqns (2.8-2.11). Results of these calculations are shown in Figures 3.5-3.10. In these figures the data points shown represent population average squared displacements, and the lines represent fits of the model to the data. Experiments in which a 10 nM concentration of either growth factor was added to cells show the largest average squared displacements, while those in which mAb 225 was added to cells appear to exhibit the lowest displacements. In calculating average squared displacements, no distinction was made between motile and immotile cells; all cells were used in the analysis.

3.3 Parameter Estimates of Speed, Persistence, and Random Motility Coefficient

To estimate speed and persistence time parameters, nonlinear, weighted curve fits were performed on population average squared displacment data. Speed and persistence time values resulting from this procedure are shown in Figures 3.11 and 3.12. Error bars represent the standard error of means. It is difficult to recognize any trends in speed and persistence time results, although all concentrations of both growth factors increase cell speed relative

to the control case and that in which receptor blocking antibody was used. Also, persistence times for experiments involving the addition of growth factors or receptor blocking antibody are lower than those seen in the control situation.

Another informative measure of cell motility is the random motility coefficient. The mathematical relationship among the random motility coefficient, speed, and persistence time is given in eqn (3.1) (Alt, 1980; Lauffenburger, 1983).

$$\mu = \frac{1}{2} S^2 P \qquad \text{(eqn 3.1)}$$

This parameter is analogous to a molecular diffusion coefficient and is useful in predicting the time-dependent displacement of a migrating cell. It represents the interaction of both speed and persistence time. Figures 3.13a-c show values of random motility coefficients as calculated for each experimental condition. These figures demonstrate, as expected from observations of curves representing population average squared displacement as a function of time (Figures 3.5-3.10), that random motility coefficients are largest for the case in which 10 nM concentrations of growth factor were added to cells and lowest when cells were incubated with mAb 225. Figures 13a and 13b indicate that cells respond to both growth factors in a dose-dependent manner, with mAb 225 serving as an inhibitor of migration. Figure 13c demonstrates that over the range of growth factor concentrations studied TGF-α is superior to EGF as a motogenic stimulant. However, data from experiments in which 1 nM concentrations of TGF-α were used lend a degree of uncertainty to this assertion.

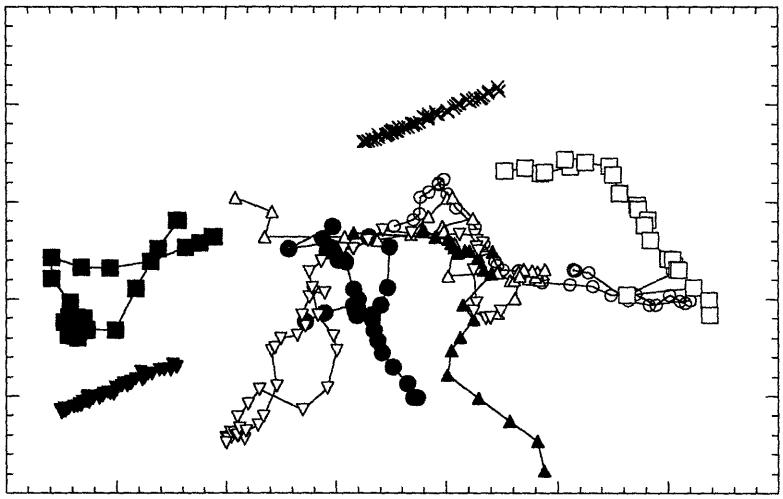

Figure 3.1 Cell paths as initially acquired from video images. The two straight, parallel tracks represent the effects of stage drift.

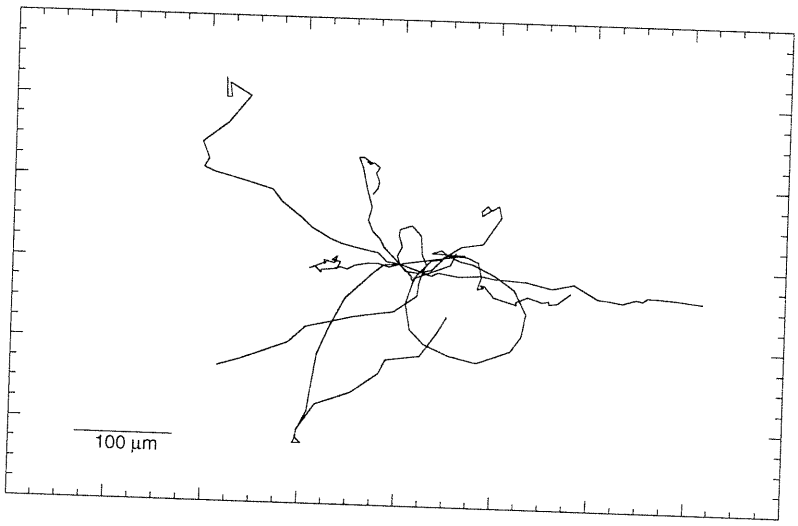

Figure 3.2 Drift-corrected cell paths.

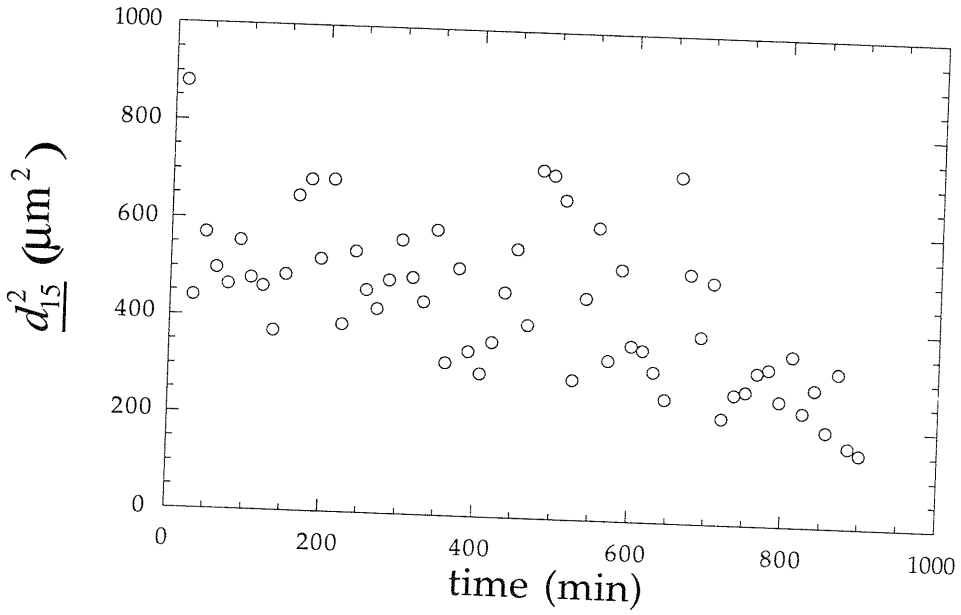

Figure 3.3 Average squared 15 minute displacements over time.

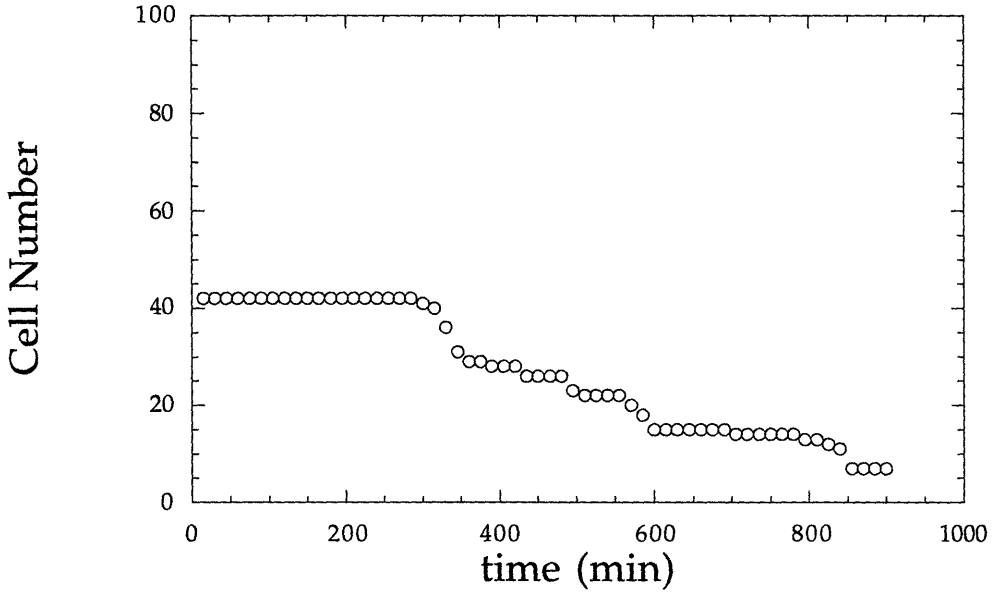

Figure 3.4 Number of cells observed over time.

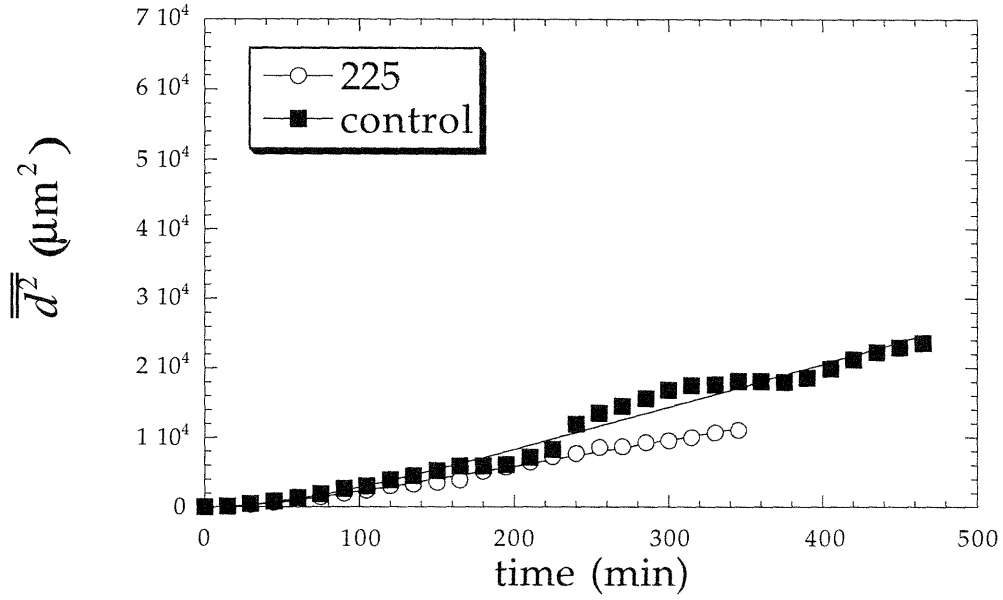

Figure 3.5 Comparison of average squared displacement of cells observed under control conditions to those which have been incubated with EGFR blocking antibody 225.

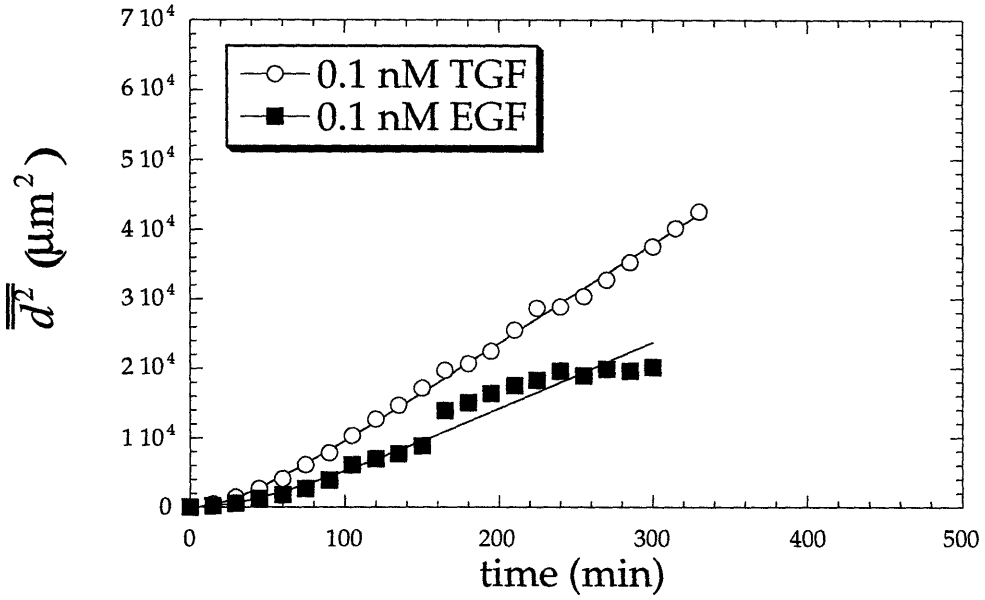

Figure 3.6 Comparison of average squared displacement of cells to which 0.1 nM TGF-α or EGF has been added.

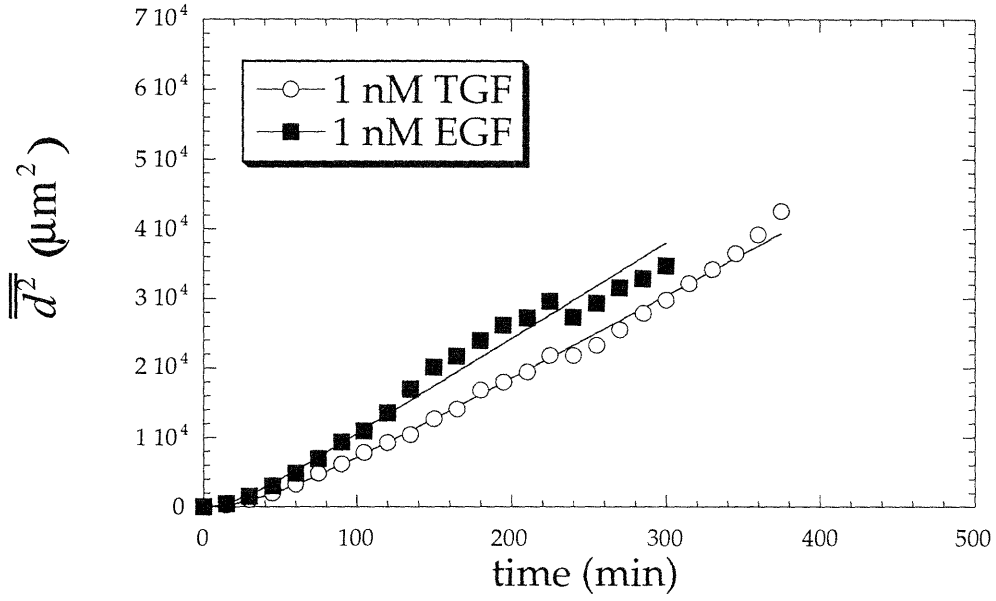

Figure 3.7 Comparison of average squared displacement of cells to which 1 nM TGF-α or EGF has been added.

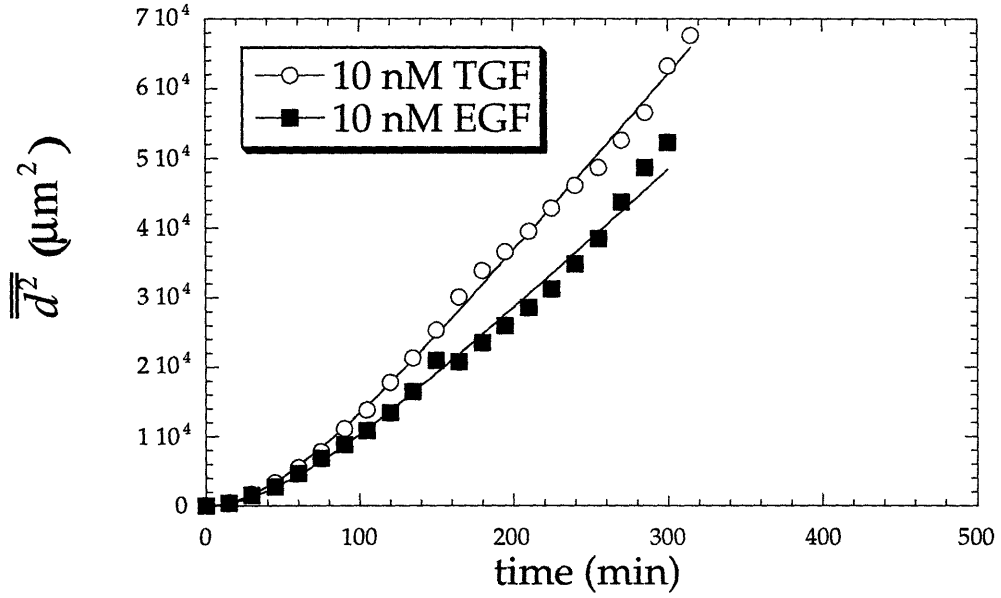

Figure 3.8 Comparison of average squared displacement of cells to which 10 nM TGF-α or EGF has been added.

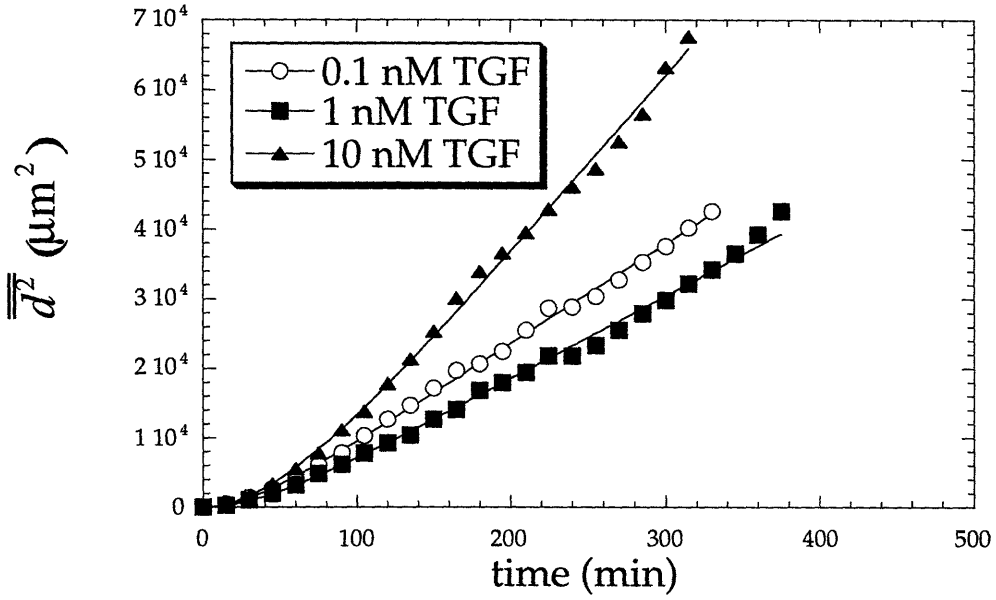

Figure 3.9 Comparison of average squared displacement of cells to which 0.1, 1, and 10 nM TGF-α have been added.

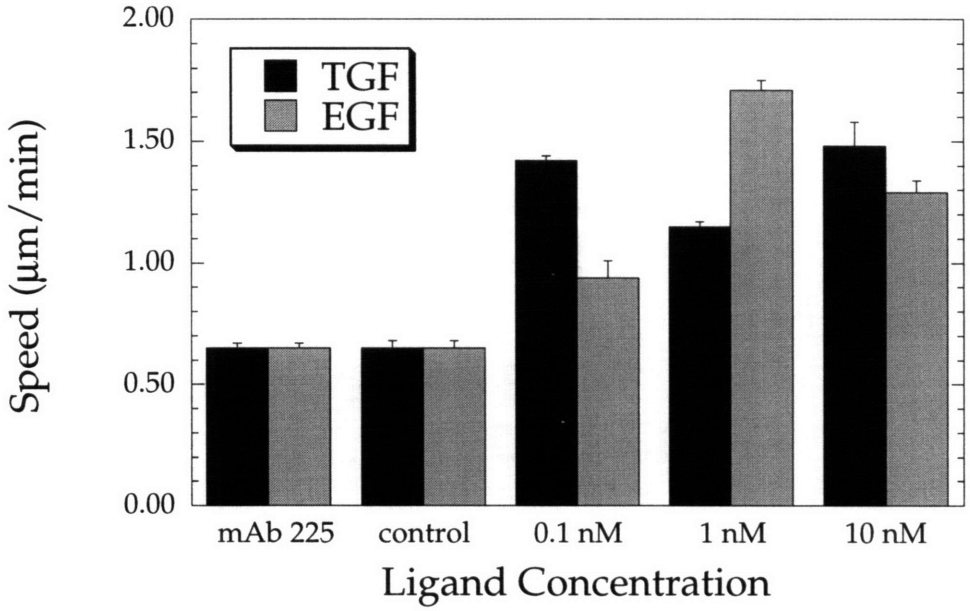

Figure 3.11 Comparison of cell speeds. Error bars represent the standard error of means.

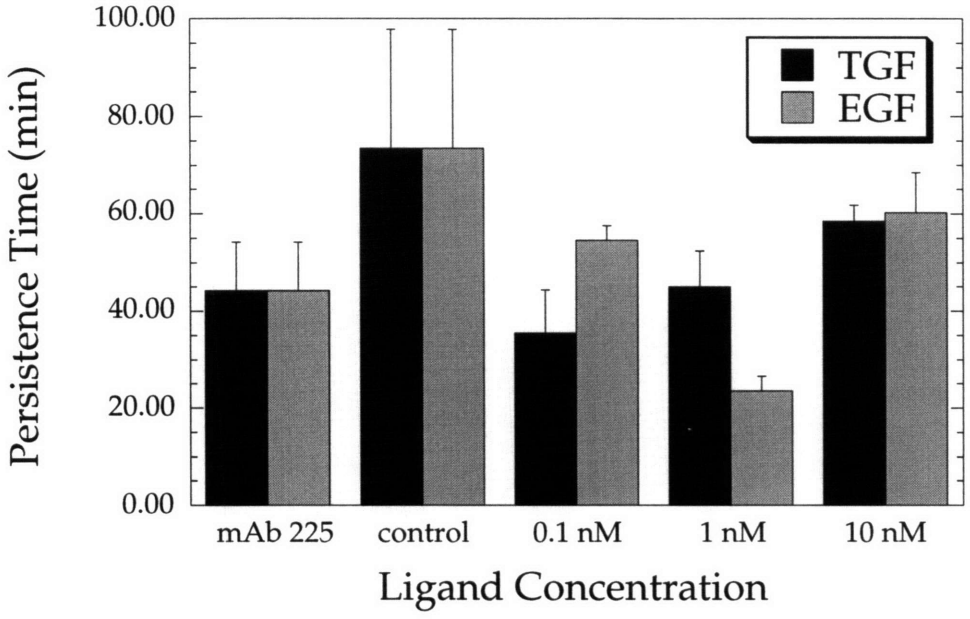

Figure 3.12 Comparison of cell persistence times. Error bars represent the standard error of means.

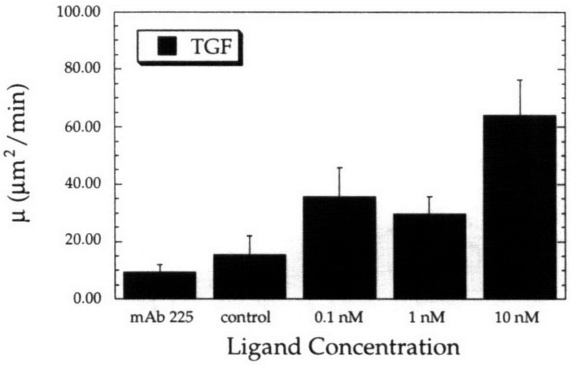

Figure 3.13a

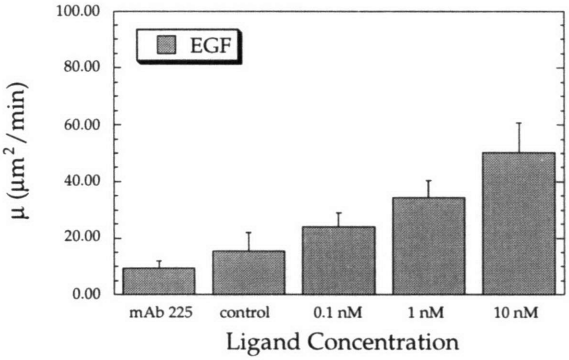

Figure 3.13b

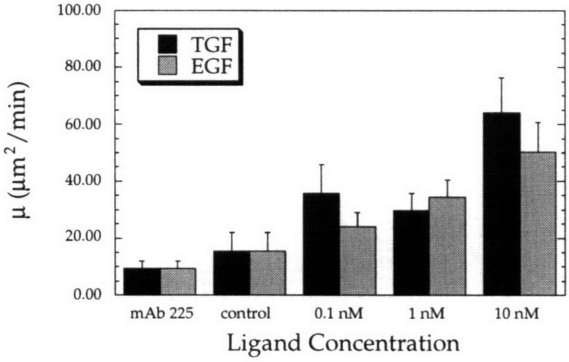

Figure 3.13c

Figures 3.13a-c Comparison of cell random motility coefficients. Error bars represent the standard error of means.

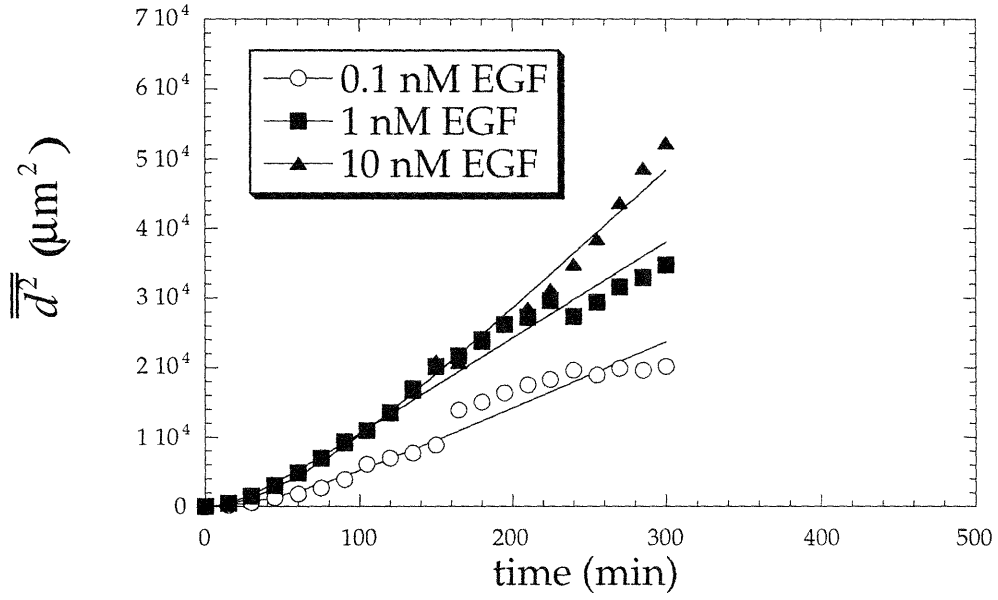

Figure 3.10 Comparison of average squared displacement of cells to which 0.1, 1, and 10 nM EGF have been added.

Chapter 4

Discussion

Both EGF and TGF-α are strong mitogenic and motogenic factors for human keratinocytes. The clinical promise of both growth factors in wound healing situations has been demonstrated (Brown et al., 1989; Schultz et al., 1987), but so far the creation of effective therapies that rely upon the activity of these, or other polypeptide growth factors, has been disappointing (reviewed by Meyer-Ingold, 1993). In designing an effective therapy around the complex interactions of growth factors and their receptors, a quantitative and predictable model of performance is desirable. The approach used in this study is designed to meet such needs.

Results indicate that both ligands significantly increase cell speed relative to control experiments and those in which EGFR blocking antibody was used. The unusually high levels of basal migration that occurred in the latter two cases are most likely a result of the stimulatory substrate used and the autocrine nature of the cells. Collagen IV, a protein which has been shown to be a particularly good stimulus for keratinocyte migration (Kim et al., 1994), was used throughout the study to provide a physiological surface upon which to observe the movement of these cells. It is thought that integrin adhesion receptors on the surface of keratinocytes, molecules that are intimately

involved in the cellular adhesion process, may also play a significant role in transducing migratory signals (Kim et al., 1994), yielding a significant level of signaling even under control conditions. Perhaps a more conclusive spread of results could be attained by using a lower concentration of the protein for migration experiments. Furthermore, keratinocytes constituitively manufacture and secrete TGF-α and HB-EGF. Secretion rates have not been characterized for these cells, but it is likely that even in the presence of receptor blocking antibody, a degree of autocrine capture of ligand occurs, generating additional migratory signals for the cells.

Motility coefficients appear to exhibit a dose-dependent response to both growth factors, with TGF-α serving as a stronger motogen than EGF. However, data from experiments in which 1 nM TGF-α was used as a stimulant lend a degree of uncertainty to this assertion. In measuring the ability of growth factors to modulate the net displacement of a cell, the random motility coefficient is most likely the variable of interest. As discussed previously (section 3.3), this parameter represents the interaction of both speed and persistence time. When considered individually, neither speed nor persistence time can be used to accurately predict net displacements, as a cell that moves with a high speed and low persistence will have the same net displacement, after a given period of time, as a cell that moves more slowly but with greater persistence.

The autocrine nature of these cells brings an additional level of interest and complexity to the analysis of their migration. A complete understanding of the mechanisms of autocrine regulation is lacking, and a major advantage of the type of analysis performed is that it allows for rigorous testing of theories

regarding the functional role of autocrine pathways as well as other migratory mechanisms.

In particular, the persistence time contains information about how a cell responds to its environment. Previous investigations of cell sensing mechanisms have focused mainly on the perception of chemotactic gradients (DeLisi et al., 1982; Tranquillo and Lauffenburger, 1986; Tranquillo and Lauffenburger, 1987; Tranquillo et al., 1988), however the persistence time is a useful measure of how a cell responds to any environmental cue. Mathematically, it is also related to parameters that describe the signaling characteristics of a cell, such as the signal response and decay time constants (Tranquillo and Lauffenburger, 1987). Unlike the case of the random motility coefficient, no trend is apparent in persistence time data. However, while not quite statistically significant ($p>0.05$), the data suggest that persistence times for all experiments in which either exogenous growth factor or receptor blocking antibody was added to cells are lower than those seen in the control situation. This observation has significant implications concerning the functional role of autocrine ligands.

Autocrine ligands are initially secreted by and subsequently bind to receptors on the same cell. As shown in Figure 4.1, in between secretion and binding steps, interaction of ligand with the cellular microenvironment allows the molecule to receive information. This information is transmitted back to the cell upon binding of the autocrine ligand. It has been proposed that the manner in which an autocrine cell secretes ligand, which then transmits environmental information back to the cell, is analogous to the emission of radio waves by sonar devices. As such, this secretion pathway and its

corresponding function have been described as "cell sonar" (personal communication, H.S. Wiley & D.A. Lauffenburger).

In the case of a migrating autocrine cell, shown in Figure 4.2, the persistent movement of the cell is assumed to be due to the symmetrical, polarized secretion and binding of an autocrine factor. Experiments designed to confirm this assumption would be particularly informative, as this model predicts that any agent perturbing the homeostasis of these autocrine loops, such as exogenous ligand or receptor blocking antibody, would diminish the persistence of the migrating, autocrine cell. Analogous to the "cell sonar" description, the cell would be essentially "blinded" by such agents. This situation is depicted in Figure 4.3. Indeed, this prediction corresponds to results obtained from this investigation. Control cells, in which autocrine loops remain unpertubed, show a higher persistence time than cells to which exogenous growth factor or receptor blocking antibody has been added.

Previous studies have highlighted the greater motogenic responsiveness of keratinocytes to TGF-α than EGF. In one study, cells were plated in the center of culture vessels, and the increase in radial size of colonies was observed to be greater in the presence of TGF-α than in the presence of EGF (Barrandon and Green, 1987). In another study, growth factor effects were screened using phagokinetic and wound healing assays, which also showed TGF-α to be a stonger motogenic agent than EGF (Cha et al., 1996). While these approaches suggest trends in the responsiveness of keratinocytes to EGF and TGF-α, they are not fundamentally quantitative in nature. Another investigation of the differential effects of EGF and TGF-α, on the stimulation of fibroblast proliferation, indicated that a range of responses could be elicited by these

ligands (Reddy et al., 1996a; Reddy et al., 1996b). Focusing on receptor/ligand trafficking dynamics, three regimes of action were shown. One in which EGF performed as a stronger mitogen, one in which TGF-α performed as a stronger mitogen, and one in which the two ligands were shown to be equipotent. The same study showed that the response could be predicted by a knowledge of whether the system was limited by the amount of available ligand, receptor downregulation, or neither. In comparing these results to the experiments performed in the present study, ELISAs have shown that ligand availability was not a determinant of the response, as no growth factor depletion was observed. Receptor levels were not quantified.

To examine trafficking dynamics further, a mathematical model describing the binding/trafficking properties of an autocrine cell was developed. Major assumptions were made concerning the trafficking properties of both EGF and TGF-α. Namely, all internalized EGF complexes were assumed to be completely degraded, and all receptors having entered the cell via a TGF-α/receptor complex were assumed to be completely recycled. Such polarized assumptions were made to accentuate the main difference between the two ligands- their intracelluar K_D. Model equations, nomenclature, and parameter values chosen are shown in Appendices A and B. Equations were solved at steady state, and ligand concentrations were assumed to be constant. Example results of this type of analysis are shown in Figure 4.4. As expected, results of this analysis indicate that over a range of ligand concentrations, exogenously added TGF-α always forms a larger number of growth factor/receptor complexes at steady state than exogenously added EGF. Assuming that the degree of migration signaling is proportional to the number of growth factor/receptor complexes, this result also predicts TGF-α

to be a stronger motogen, over all ligand concentrations. The random motility coefficients obtained from this study confirm this behavior. Other approaches explaining the differential effects of EGF and TGF-α have focused on the possibility of differential signaling pathways of receptor tyrosine kinases. In support of this theory, a limited number of differences in Western blots, prepared to examine the magnitude and kinetics of tyrosine phosphorylation as induced by EGF and TGF-α, suggested different signaling activities of the two ligands (Cha et al., 1996). Another study demonstrated a correlation between growth factor specificity and matrix metalloproteinase activity, as assayed by gelatin zymography (McCawley et al., 1996). These results are encouraging, but not quantiatively conclusive. The *in vivo* cellular response most likely involves a combination of differential trafficking and signaling pathways, however additional study will be necessary to fully appreciate the complexity of such interactions.

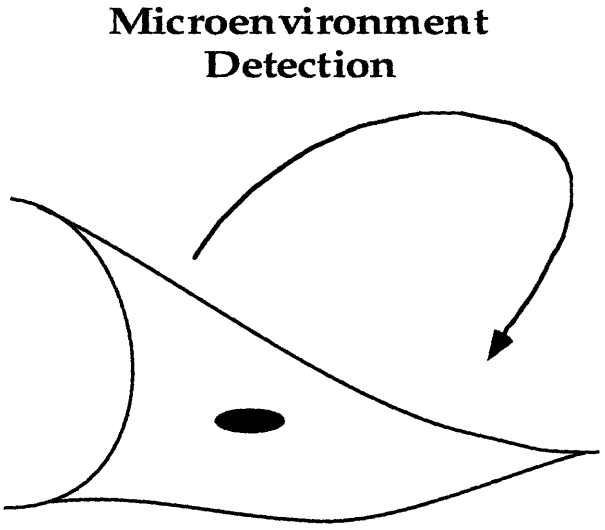

Figure 4.1 An autocrine cell sensing its local microenvironment (adapted from H.S. Wiley).

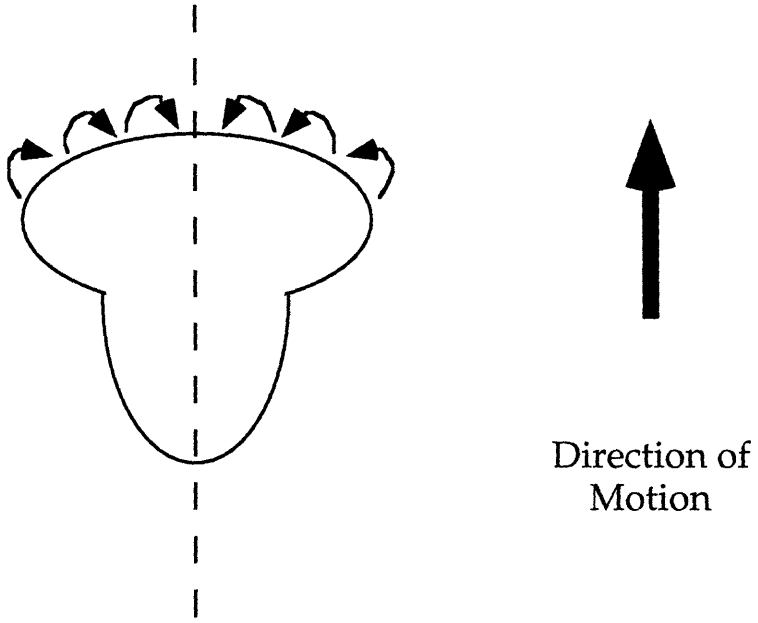

Figure 4.2 A persistent autocrine cell (adapted from Tranquillo and Lauffenburger, 1987). Curved arrows represent stimulation by autocrine ligand at the leading edge of the migrating cell.

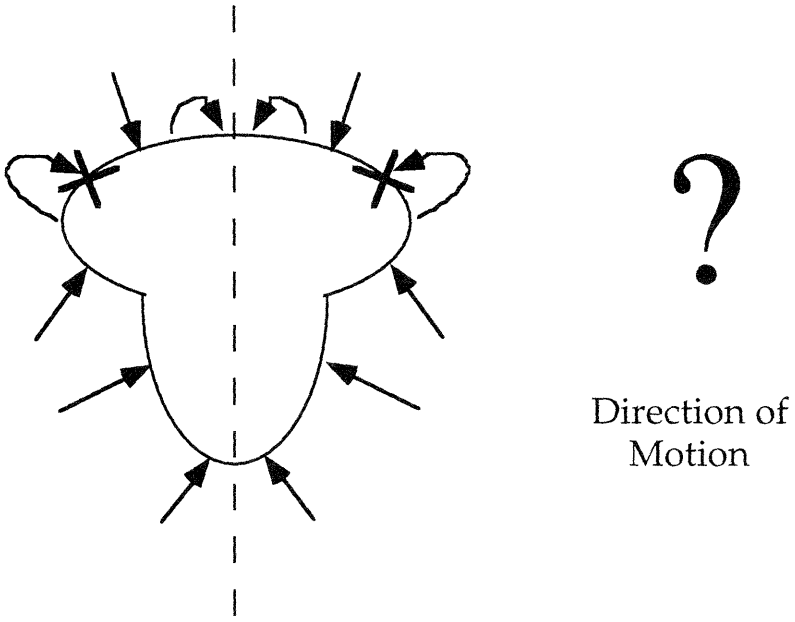

Figure 4.3 The disrupted migration of an autocrine cell (adapted from Tranquillo and Lauffenburger, 1987). Curved arrows represent stimulation by autocrine ligand at the leading edge of the migrating cell, straight arrows represent stimulation by exogenous ligand, and X's represent the action of EGFR blocking antibodies.

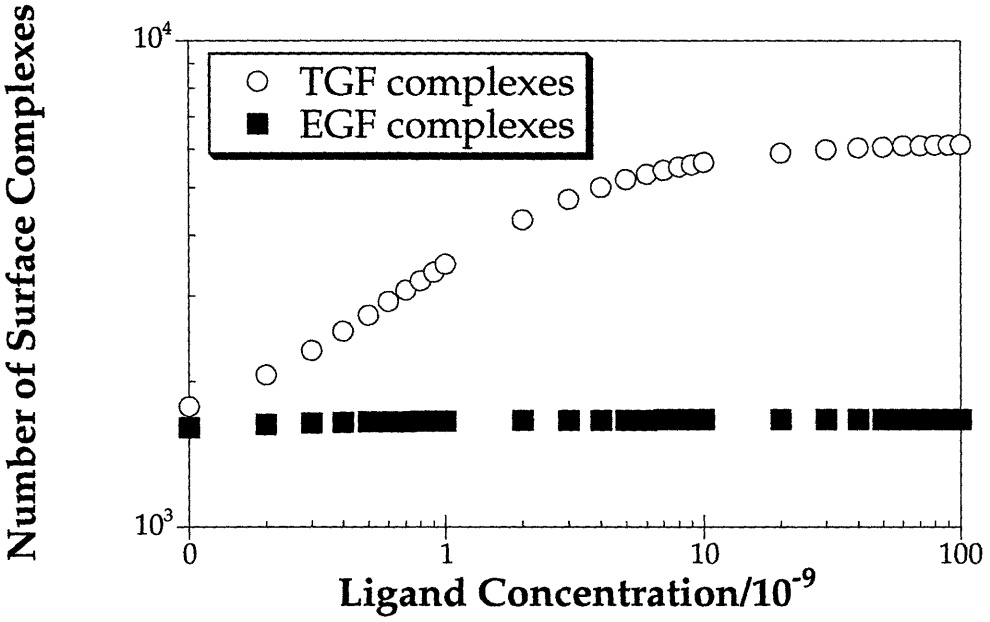

Figure 4.4 Model Results. Results were obtained from parameter values reflecting a condition of low cell density and autocrine secretion.

Appendix A

$$\frac{dR_s}{dt} = -k_f^{TGF} R_s (L_{exog}^{TGF} + (1-f)\frac{\rho A Q}{N_{Av} V}\int_0^t dt)$$
$$-k_f^{EGF} R_s L_{exog}^{EGF} + k_r^{TGF} C_s^{TGF} + k_r^{EGF} C_s^{EGF}$$
$$-k_{eR} R_s + k_{rec} R_i (1-f_{deg}) + V_s - fQ \qquad \text{(eqn A.1)}$$

$$\frac{dC_s^{TGF}}{dt} = +k_f^{TGF} R_s (L_{exog}^{TGF} + (1-f)\frac{\rho A Q}{N_{Av} V}\int_0^t dt)$$
$$-k_r^{TGF} C_s^{TGF} - k_{eC} C_s^{TGF} + fQ \qquad \text{(eqn A.2)}$$

$$\frac{dC_s^{EGF}}{dt} = +k_f^{EGF} R_s L_{exog}^{EGF} - k_r^{EGF} C_s^{EGF} - k_{eC} C_s^{EGF} \qquad \text{(eqn A.3)}$$

$$\frac{dR_i}{dt} = +k_{eR} R_s + k_{eC} C_s^{TGF}$$
$$-R_i (k_{deg} f_{deg} + k_{rec}(1-f_{deg})) \qquad \text{(eqn A.4)}$$

Appendix B

Model Nomenclature	Parameter Values
A = total area of cell culture dish (cm^2)	0.35
C_s^{TGF} = surface complexes bound to TGF - α (# $cell^{-1}$)	
C_s^{EGF} = surface complexes bound to EGF (# $cell^{-1}$)	
f = autocrine capture probability for TGF - α	0.1
k_{eC} = internalization rate constant for complexes (min^{-1})	0.3
k_{eR} = internalization rate constant for free receptors (min^{-1})	0.03
k_{deg} = internal receptor degration rate constant (min^{-1})	2.2e-3
k_f^{TGF} = forward binding rate constant for TGF - α (M^{-1} min^{-1})	4.3e7
k_f^{EGF} = forward binding rate constant for EGF (M^{-1} min^{-1})	6.3e7
k_r^{TGF} = reverse binding rate constant for TGF - α (min^{-1})	0.27
k_r^{EGF} = reverse binding rate constant for EGF (min^{-1})	0.16
k_{rec} = recycling rate constant (min^{-1})	5.8e-2
L_{exog}^{EGF} = exogenous EGF concentration (M)	
L_{exog}^{TGF} = exogenous TGF - α concentration (M)	
N_{Av} = Avagadro' s number (# mol^{-1})	
ρ = plated cell density (cells cm^{-2})	7143
Q = TGF - α autocrine secretion rate (# $cell^{-1}$ min^{-1})	8026
R_i = Total internal free receptors (# $cell^{-1}$)	
t = duration of experiment (min)	1440
V = volume of culture media above cells (L)	0.004
V_s = free receptor synthesis rate (# $cell^{-1}$ min^{-1})	100

References

Aaronson, S. (1991). Growth Factors and Cancer. Science *245*, 1146-1152.

Alt, W. (1980). Biased Random Walk Models for Chemotaxis and Related Diffusion Approximation. J. Math. Biol. *9*, 147-177.

Bade, E. G., and Nitzgen, B. (1985). Extracellular Matrix (ECM) Modulates the EGF-Induced Migration of Liver Epithelial Cells in Serum-Free, Hormone-Supplemented Medium. In Vitro Cell Dev. Biol. *21*, 245-248.

Barrandon, Y., and Green, H. (1987). Cell Migration Is Essential for Sustained Growth of Keratinocyte Colonies: The Roles of Transforming Growth Factor-Alpha and Epidermal Growth Factor. Cell *50*, 1131-1137.

Bates, S. E., Davidson, N. E., et al. (1988). Expression of Transforming Growth Factor-alpha and its Messenger Ribonucleic Acid in Human Breast Cancer: its Regulation by Estrogen and its Possible Functional Significance. Mol. Endocrinol. *2*, 543-555.

Beauchamp, R. D., Barnard, J. A., et al. (1989). Localization of Transforming Growth Factor-alpha and its Receptor in Gastric Mucosal Cells. J. Clin. Invest. *84*, 1017-1023.

Brachmann, R., Lindquist, P. B., et al. (1989). Transmembrane TGF-alpha Precursors Activate EGF/TGF-alpha Receptors. Cell *56*, 691-700.

Bringman, T. S., Lindquist, P. B., et al. (1987). Different Transforming Growth Factor-alpha Species are Derived from a Glycosylated and Palmitoylated Transmembrane Precursor. Cell *48*, 429-440.

Brown, G. L., Nanney, L. B., et al. (1989). Enhancement of Wound Healing by Topical Treatment with Epidermal Growth Factor. N. Engl. J. Med., 76-79.

Burgess, A. W. (1989). Epidermal Growth Factor and Transforming Growth Factor alpha. Brit. Med. Bull. *45*, 401-424.

Carpenter, G., and Cohen, S. (1990). Epidermal Growth Factor. J. Biol. Chem. *265*, 7709-7712.

Carpenter, G., and Wahl, M. I. (1990). The Epidermal Growth Factor Family. In Peptide Growth Factors and Their Receptors, M. B. Sporn and A. B. Roberts, eds. (Berlin: Springer-Verlag), pp. 69-171.

Cha, D., O'Brien, P., et al. (1996). Enhanced Modulation of Keratinocyte Motility by Transforming Growth Factor-alpha relative to Epidermal Growth Factor. J. Invest. Dermatol. *106*, 1-8.

Chang, C.-P., Lazar, C. S., et al. (1993). Ligand-indiced Internalization of the Epidermal Growth Factor Receptor Is Mediated by Multiple Endocytic Codes Analogous to the Tyrosine Motif Found in Constitutively Internalized Receptors. J. Biol. Chem. *268*, 19312-19320.

Clark, R. A. (1993). Basics of Cutaneous Wound Repair. J. Dermatol. Surg. Oncol. *19*, 693-706.

Coffey, R. J., Derynck, R., et al. (1987). Production and Auto-Induction of Tranforming Growth Factor-alpha in Human Keratinocytes. Nature *328*, 817-820.

DeLisi, C., Marchetti, F., et al. (1982). A Theory of Measurement Error and its Implications for Spatial and Temporal Gradient Sensing During Chemotaxis. Cell Biophys. *4*, 211-229.

Derynck, R. (1992). The Physiology of Transforming Growth Factor-alpha. Advanc. Cancer Res. *58*, 27-52.

Derynck, R., Goeddel, D. V., et al. (1987). Synthesis of mRNAs for Transforming Growth Factors-alpha and -beta and the Epidermal Growth Factor Receptor by Human Tumors. Cancer Res. *47*, 707-712.

Dickinson, R. B., and Tranquillo, R. T. (1993). Optimal Estimation of Cell Movement Indices from the Statistical Analysis of Cell Tracking Data. AIChE J. *39*, 1995-2012.

DiMilla, P. A., Quinn, J. A., et al. (1992). Measurement of Individual Cell Migration Parameters for Human Tissue Cells. AIChe J. *38*, 1092-1104.

Dominey, A. M., Wang, X.-J., et al. (1993). Targeted Overexpression of Transforming Growth Factor Alhpa in the Epidermis of Transgenic Mice Elicits Hyperplasia, Hyperkeratosis, and Spontaneous, Squamous Papillomas. Cell Growth Diff. *4*, 1071-1082.

Dunn, G. A. (1983). Characterising a Kinesis Response: Time Average Measures of Cell Speed and Directional Persistence. Agents and Actions Suppl. *12*, 14-33.

Ebner, R., and Derynck, R. (1991). Epidermal growth factor and transforming growth factor-alpha: differential intracellular routing and processing of ligand-receptor complexes. Cell Reg. *2*, 599-612.

French, A. R., and Lauffenburger, D. A. (1996). Intracellular Receptor/Ligand Sorting Based on Endosomal Retention Components. Biotechnology and Bioengineering *In Press*.

French, A. R., Tadaki, D. K., et al. (1995). Intracellular Trafficking of Epidermal Growth Factor Family Ligands is Directly Influenced by the pH Sensitivity of the Receptor/Ligand Interaction. J. Biol. Chem. *270*, 4334-4340.

Goodman, S. L., Risse, G., et al. (1989). The E8 Subfragment of Laminin Promotes Locomotion of Myoblasts Over Extracellular Matrix. J. Cell Biol. *109*, 799.

Gospodarowicz, D. (1981). Epidermal and Nerve Gowth Factors in Mammalian Development. Ann. Rev. Physiol. *43*, 251-263.

Gray, A., Dull, T. J., et al. (1983). Nucleotide Sequence of Epidermal Growth Factor cDNA Predicts a 128,000-Molecular Weight Protein Precursor. Nature *303*, 722-725.

Hashimoto, K., Higashiyama, S., et al. (1994). Heparin-Binding Epidermal Growth Factor-Like Growth Factor is an Autocrine Growth Factor for Human Keratinocytes. J. Biol. Chem. *269*, 20060-20066.

Hudson, L. G., and Gill, G. N. (1991). Regulation of Gene Expression by Epidermal Growth Factor. In Genetic Engineering, J. K. Setlow, ed. (New York: Plenum Press), pp. 137-151.

Kawamoto, T., Sato, J. D., et al. (1983). Growth stimulation of A431 cells by erpidermal growth factor: Identification of high-affinity receptors for epidermal growth factor by an anti-receptor monoclonal antibody. Proc. Natl. Acad. Sci. USA *80*, 1337-1341.

Khazaie, K., Schirrmacher, V., et al. (1993). EGF Receptor in Neoplasia and Metastasis. Can. Met. Rev. *12*, 255-274.

Kim, J. P., Chen, J. D., et al. (1994). Human Keratinocyte Migration on Type IV Collagen. Lab. Invest. *71*, 401-408.

Kobrin, M. S., Samsoondar, J., et al. (1988). Transforming Growth Factor Secreted by Untransformed Bovine Anterior Pituitary Cells in Culture. II. Identification Using a Sequence-Specific Monoclonal Antibody. J. Biol. Chem. *261*, 14414-14419.

Lauffenburger, D. A. (1983). Measurement of Phenomenological Parameters for Leukocyte Motility and Chemotaxis. Agents and Actions Suppl. *12*, 34-53.

Lee, D. C., Fenton, S. E., et al. (1995). Transforming Growth Factor Alpha: Expression, Regulation, and Biological Activites. Pharm. Rev. *47*, 51-85.

Madtes, D. K., Raines, E. W., et al. (1988). Induction of Transforming Growth Factor-alpha in Activated Human Alveolar Macrophages. Cell *53*, 285-293.

Manske, M., and Bade, E. G. (1994). Growth Factor-Induced Cell Migration: Biology and Methods of Analysis. In International Review of Cytology: A Survey of Cell Biology, K. W. Jeon and J. Jarvik, eds. (San Diego: Academic Press), pp. 49-96.

Massague, J. (1983). Epidermal Growth Factor-like Transforming Growth Factor. J. Biol. Chem. *258*, 13614-13620.

Massague, J. (1990). Transforming Growth Factor-Alpha. J. Biol. Chem. *265*, 21393-21396.

Massague, J., and Pandiella, A. (1993). Membrane-Anchored Growth Factors. Annu. Rev. Biochem. *62*, 515-541.

McCawley, L. J., O'Brien, P., et al. (1996). Receptor Tyrosine Kinase Specificity in the Mediation of Keratinocyte Motility and Invasive Potential. submitted, ?

Meyer-Ingold, W. (1993). Wound Therapy: Growth Factors as Agents to Promote Healing. TIBtech. *11*, 387-392.

Nister, M., Libermann, T. A., et al. (1988). Expression of messenger RNAs for Platelete-Derived Growth Factor and Transforming Growth Factor-alpha and their receptors in Human Glioma Cell Lines. Cancer Res. *48*, 3910-3918.

Othmer, H. G., Dunbar, S. R., et al. (1988). Models of Dispersal in Biological Systems. J. Math. Biol. *26*, 263-298.

Pimentel, E. (1994). Handbook of Growth Factors Volume 2: Peptide Growth Factors (Boca Raton: CRC Press).

Pittelkow, M. R., Cook, P. W., et al. (1993). Autonomous Growth Factor of Human Keratinocytes Requires Epidermal Growth Factor Receptor Occupancy. Cell Growth Diff. *4*, 513-521.

Rappolee, D. A., Mark, D., et al. (1988). Wound Macrophages Express TGF-aplpha and Other Growth Factors In Vivo: Analysis by mRNA Phenotyping. Science *241*, 708-712.

Reddy, C., Wells, A., et al. (1996a). Differential EGF Receptor Trafficking Influences Relative Mitogenic Potencies of Epidermal Growth Factor and Transforming Growth Factor-Alpha. submitted J. Cell. Physiol.

Reddy, C. C., Weels, A., et al. (1996b). Receptor-Mediated Effects on Ligand Availablity Influence Relative Mitogenic Potencies of Epidermal Growth Factor and Transforming Growth Fator Alpha. J. Cell. Physiol. *166*, 512-522.

Sato, J. D., Kawamoto, T., et al. (1983). Mol. Biol. Med. *1*, 511.

Sato, J. D., Le, A. D., et al. (1987). Derivation and Assay of Biological Effects of Monoclonal Antibodies to Epidermal Growth Factor Receptors. Meth. Enzymol. *146*, 63-81.

Schreiber, A. B., Winkler, M. E., et al. (1986). Transforming Growth Factor-alpha: A More Potent Angiogenic Mediator Than Epidermal Growth Factor. Science *232*, 1250-1253.

Schultz, G. S., White, M., et al. (1987). Epithelial Wound Healing Enhanced by Transforming Growth Factor-alpha and Vaccinia Growth Factor. Science *235*, 350-352.

Soler, C., and Carpenter, G. (1994). The Epidermal Growth Factor Family. In Guidebook to Cytokines and Their Receptors, N. Nicola, ed. (Oxford: Oxford University Press), pp. 194-197.

Tranquillo, R. T., and Lauffenburger, D. A. (1986). Consequences of Chemosensory Phenomena for Leukocyte Chemotactic Orientation. Cell Biophysics *8*, 1-46.

Tranquillo, R. T., and Lauffenburger, D. A. (1987). Stochastic Model of Leukocyte Chemosensory Movement. J. Math. Biol. *25*, 229-262.

Tranquillo, R. T., Lauffenburger, D. A., et al. (1988). A Stochastic Model for Leukocyte Random Motility and Chemotaxis Based on Receptor Binding Fluctuations. J. Cell Biol. *106*, 303-309.

Valverius, E. B., Bates, S. E., et al. (1989). Transforming Growth Factor-alpha Production and Epidermal Growth Factor Expression in Normal and Oncogene Transformed Human Mammary Epithelial Cells. Mol. Endocrinol. *3*, 203-214.

van der Geer, P., Hunter, T., et al. (1994). Receptor Protein-Tyrosine Kinases And Their Signal Transduction Pathways. Annu. Rev. Cell. Biol. *10*, 251-337.

Wells, A. (1988). The EGFR & its Ligands. In Oncogenes, C. Benz and E. Lui, eds. (Boston: Academic Publishers), pp. 143-168.

Wilcox, J. N., and Derynck, R. (1988). Localization of Cells Synthesizing Transforming Growth Factor-alpha mRNA in the Mouse Brain. J. Neurosci. *8*, 1901-1904.

Winter, G. D. (1962). Formation of the Scab and the rate of Epithelialization of Superficial Wounds in the Skin of the Young Domestic Pig. Nature *193*, 293-294.

Wong, S. T., Winchell, L. F., et al. (1989). The TGF-alpha Precursor Expressed on the Cell Suface Binds to the EGF Receptor on Adjacent Cell, Leading to Signal Transduction. Cell *56*, 495-506.

Yaoita, H., Foidart, J. M., et al. (1978). Localization of the Collagenous Componenet in Skin Basement Membrane. J. Invest. Dermatol. *70*, 191-193.